JACS
JOURNAL OF THE AMERICAN CHEMICAL SOCIETY
pubs.acs.org/JACS

Article

Modular Synthetic Platform for the Elaboration of Fragments in Three Dimensions for Fragment-Based Drug Discovery

Andres R. Gomez-Angel,[§] Hanna F. Klein,[§] Stephen Y. Yao,[§] James R. Donald, James D. Firth, Rebecca Appiani, Cameron J. Palmer, Joshua Lincoln, Simon C. C. Lucas, Lucia Fusani, R. Ian Storer, and Peter O'Brien*

Cite This: https://doi.org/10.1021/jacs.5c08786

Read Online

ACCESS | Metrics & More | Article Recommendations | Supporting Information

ABSTRACT: Fragment-based drug discovery (FBDD) is a key strategy employed in the hit-to-lead phase of pharmaceutical development. The rate-limiting step of this process is often identifying and optimizing synthetic chemistry suitable for fragment elaboration, especially in three dimensions (3-D). To address this limitation, we herein present a modular platform for the systematic and programmable elaboration of two-dimensional (2-D) fragment hits into lead-like 3-D compounds, utilizing nine bifunctional building blocks that explore a range of vectors in 3-D. The building blocks comprise (i) rigid sp^3-rich bicyclic cyclopropane-based structures to fix the vectors and (ii) two synthetic handles—a protected cyclic amine and a cyclopropyl *N*-methyliminodiacetic acid (MIDA) boronate. To validate our approach, we present (i) multigram-scale synthesis of each 3-D building block; (ii) Suzuki-Miyaura cross-coupling reactions of the cyclopropyl BMIDA functionality with aryl bromides; and (iii) *N*-functionalization (via commonplace medicinal chemistry toolkit reactions) of arylated products to deliver 3-D lead-like compounds. Each building block accesses a distinct 3-D exit vector, as shown by analysis of the lowest energy conformations of lead-like molecules using RDKit, and by X-ray crystallography of pyrimidine methanesulfonamide derivatives. Since the synthetic methodology is established in advance of fragment screening and utilizes robust chemistry, the elaboration of fragment hits in 3-D for biochemical screening can be achieved rapidly. To provide proof-of-concept, starting from the drug Ritlecitinib, the development of inhibitors of Janus kinase 3 (JAK3) around a putative pyrrolopyrimidine 2-D fragment hit was explored, streamlining the discovery of a novel and selective JAK3 inhibitor with IC_{50} = 69 nM.

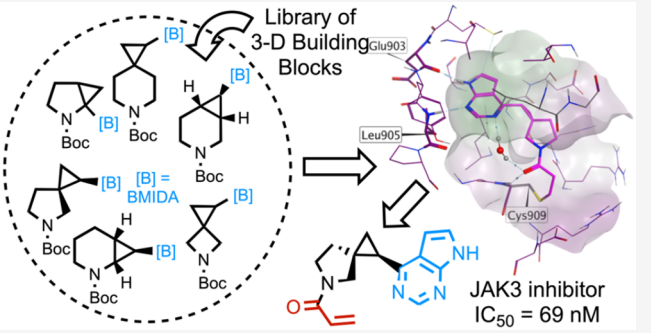

INTRODUCTION

Fragment-based drug discovery (FBDD) has developed into a mature technology for the identification of low molecular weight hits against protein targets and subsequent progression to lead candidates.[1−5] Indeed, eight drugs, along with over 59 additional clinical candidates, have originated from FBDD programs.[6,7] Due to the low molecular weight (MW) of fragments (MW typically <300 Da),[8] establishing and employing a fragment library that can effectively sample chemical space (typically a few thousand compounds) is far cheaper and more straightforward than utilizing a high-throughput screening library.[3,4,9] This is perhaps one of the reasons for its popularity. A key part of FBDD is "growing" or "elaborating" fragment hits (often guided by X-ray crystallographic studies) to increase the potency and to obtain lead compounds. It is often desirable that this fragment growth can be performed along multiple vectors in 3-D space, potentially from sp3 carbons, allowing the synthesis of 3-D lead-like molecules with associated desirable physicochemical properties.[10,11] However, fragment growth is often limited to commercially available structural analogs of fragment hits, and even seemingly simple fragment growth design ideas can require de novo synthetic strategies. Further limitations can arise from the focus of medicinal chemists on a small toolkit of reactions, especially the formation of sp^2−sp^2 (aryl−aryl) C−C bonds.[12,13] For these reasons, synthetic organic chemistry has been highlighted as the rate-limiting step in the fragment growth/elaboration stage,[14,15] and this led to a call from FBDD industrial practitioners to academia to develop methods to allow the synthetic "elaboration of fragments in three dimensions from many different growth points/vectors using methodology that is worked out prior to fragment screening."[14]

Received: May 26, 2025
Revised: June 29, 2025
Accepted: July 18, 2025

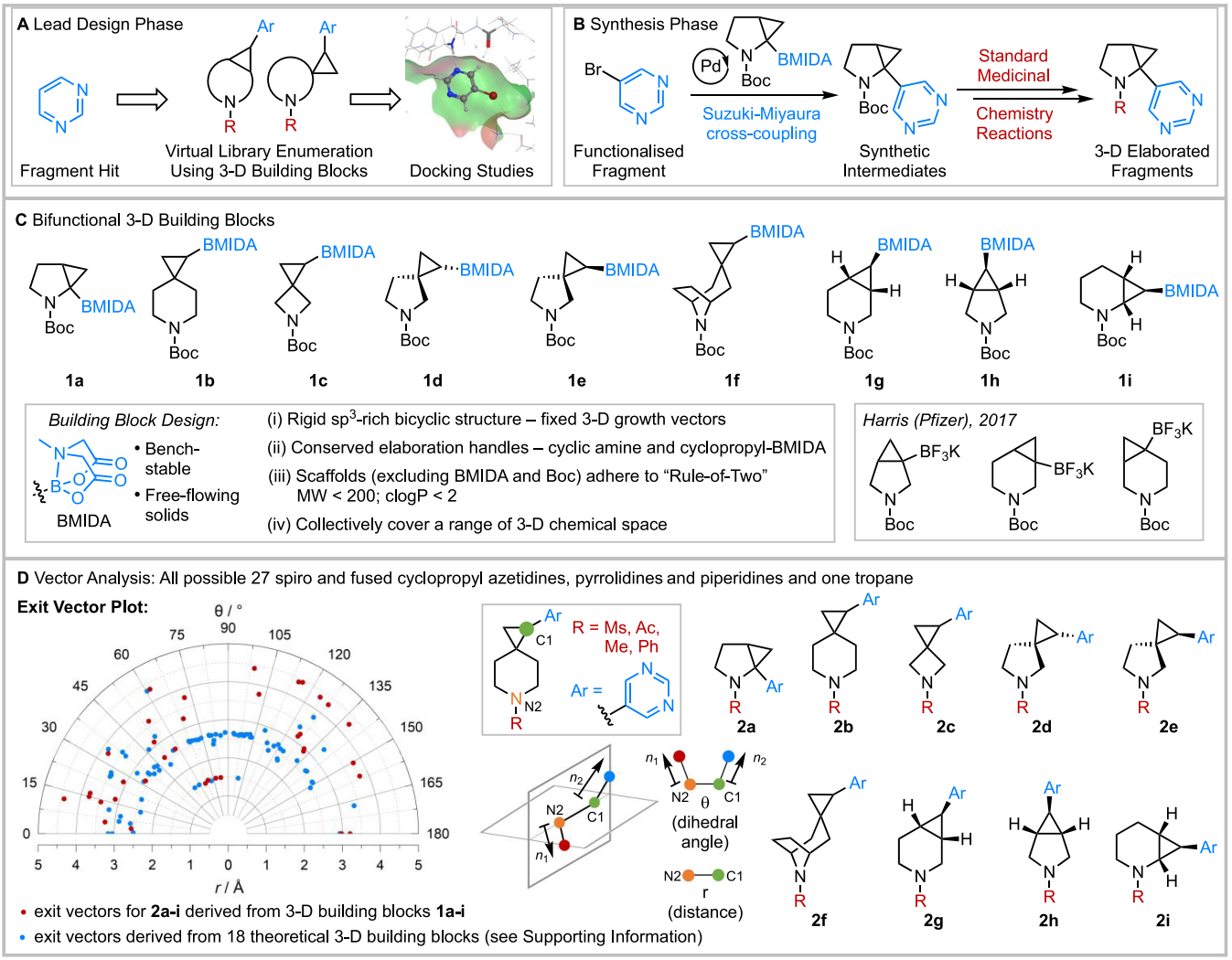

Figure 1. Modular synthetic platform for fragment elaboration in 3-D and the design and analysis of 3-D building blocks. (A) Lead design phase. (B) Synthesis phase. (C) Bifunctional 3-D building blocks. (D) Exit vector analysis and exit vector plot (where applicable, only one enantiomeric series for each compound is displayed on the exit vector plot).

One approach to achieve this goal is the development of new fragments with accompanying synthetic methodology that facilitates growth along multiple vectors.[16] However, this approach requires significant up-front investment of synthetic chemistry resources, as highlighted in our previous work on 3-D fragment libraries.[17−20] A second approach would be the direct growth of existing fragments along non-traditional vectors through C−H activation methods that are site-selective for different growth points on a fragment, while being robust enough to be compatible with essential polar functionality.[21−24] In both of these contexts, the term "fragment sociability" has been identified to distinguish between fragments for which fragment elaboration is synthetically enabled ("sociable") from those where it is not ("unsociable").[25] Despite some progress in both of these approaches, the extensive structural diversity presented by 3-D molecular architectures, the polar functionalities required in medicinal chemistry settings, and the speed with which drug discovery projects move forward mean that progress has been slow and such a synthetic ideal for fragment elaboration currently remains elusive.

As a result, we propose a different approach, namely, the development of a modular synthetic platform that would enable the systematic and programmable elaboration of typically 2-D fragment hits into 3-D lead-like compounds. This alternative approach should enable fragment elaboration across a range of 3-D vectors, and key features are captured in Figure 1A,1B. Rather than the development of complex elaboration methodology for each fragment class prior to screening, our approach utilizes the power and robustness of the limited, but reliable, toolkit of reactions that are commonly employed in medicinal chemistry.[12,13,26] This, together with a newly designed collection of bifunctional 3-D building blocks **1a-i** (Figure 1C) equipped with distinct vectors (vide infra), will enable the rapid and systematic fragment growth of 2-D fragments hits.

The approach, which is best suited to working with proteins that are structurally enabled, begins with the lead design phase (Figure 1A). For example, consider that pyrimidine is a fragment hit against the protein target of interest and binding has been confirmed by X-ray crystallography. The set of 3-D building blocks **1a-i** (Figure 1C) can then be used to enumerate a virtual library of 3-D lead-like compounds in which the pyrimidine fragment hit (blue) has been diversified with the building blocks and typical medicinal chemistry capping groups (red) to pick up additional protein binding

https://doi.org/10.1021/jacs.5c08786
J. Am. Chem. Soc. XXXX, XXX, XXX−XXX

interactions. Computational docking studies of this virtual library will then reveal a set of potential lead-like molecules for synthesis comprising the pyrimidine fragment (blue) and 3-D building block linker scaffolds that display the additional binding groups (red) along the 3-D vector provided by each building block. Next, there are two parts to the synthesis phase (Figure 1B). First, elaboration of the pyrimidine fragment hit (blue) will be performed by cross-coupling a commercially available brominated analog, 3-bromopyrimidine in this case, with the selected 3-D building blocks, illustrated with **1a**. Second, after Boc group removal, *N*-functionalization will be carried out to place the capping groups (red) in particular 3-D vectors relative to the initial fragment hit (blue). We envisioned that both stages of the synthesis phase would utilize reactions that are robust and widely used in medicinal chemistry to minimize any barriers to uptake by FBDD practitioners; *N*-functionalization using amide/sulfonamide formation, Buchwald-Hartwig cross-coupling, S_NAr (nucleophilic aromatic substitution), and reductive amination have been used in this work. Since the synthetic methodology is established in advance of fragment screening and utilizes the same set of reactions, the generation of fragment hits that are elaborated in 3-D for biochemical screening can be achieved rapidly. After these initial screening results, the process can be applied iteratively to further optimize the compounds.

The utility of our approach hinges on the availability of a collection of synthetically enabled bifunctional building blocks that access a range of 3-D vectors and 3-D chemical space. With this in mind, we designed the set of 3-D building blocks **1a-i** shown in Figure 1C using the following criteria: (i) they have a rigid sp^3-rich bicyclic structure (fused or spirocyclic) comprising a cyclopropane[27,28] to fix the 3-D vectors between the fragment and the *N*-capping groups (vide infra); (ii) they are equipped with the same two synthetic handles, namely, a Boc-protected cyclic amine and a cyclopropyl *N*-methyliminodiacetic acid (MIDA) boronate;[29] (iii) the scaffolds (i.e., excluding the BMIDA and Boc groups) have suitable physicochemical properties, achieved by adhering to AstraZeneca's "Rule-of-Two" guidelines for medicinal chemistry building blocks[30] (MW < 200; clogP < 2); and (iv) they cover, collectively, a range of 3-D chemical space (vide infra).

The incorporation of cyclopropyl MIDA boronates into 3-D building blocks **1a-i** as the fragment elaboration handle is strategic. First, since many fragment libraries contain a high proportion of aryl and heteroaryl compounds, it was envisaged that any such fragment hit could be elaborated from a halogenated analog (including FragLites which are a screening set of ∼ 30 medicinally relevant aryl bromides and iodides[31,32]) using well-established, reliable Suzuki-Miyaura cross-coupling (Figure 1B, synthesis phase).[33−38] Second, MIDA boronates are known to be bench-stable, free-flowing crystalline solids that can be easily purified, making them ideal linchpin building blocks, as shown by Burke's automated syntheses.[29] At the outset of our project, the closest structural analogs to 3-D building blocks **1a-i** were fused cyclopropyl pyrrolidine and piperidine BF_3K salts reported by Harris et al. at Pfizer[39] (Figure 1C), which were not designed with fragment elaboration in mind, and difluorocyclopropane analogs of **1b**, **1c** and Harris' fused piperidines, as described by Grygorenko et al.[40] After the development of our synthetic routes to racemic 3-D building blocks **1a-i** (excluding **1h** which is a *meso* compound), Gutiérrez-Bonet, Popov and co-workers at Merck reported the asymmetric synthesis of cyclopropyl boronate analogs of **1c** and Harris' cyclopropyl pyrrolidine and piperidine BF_3K salts.[38]

A key design feature of 3-D building blocks **1a-i** was that they would provide a range of 3-D vectors and 3-D chemical space coverage (Figure 1D). For this, 3-D vector analysis was carried out by enumeration of relevant chemical space in tandem with Grygorenko's exit vector plot analysis.[41,42] To start, virtual 3-D bifunctional building blocks comprising all 26 possible combinations of a cyclic amine (derived from azetidine, pyrrolidine or piperidine) and a fused or spirocyclic cyclopropyl BMIDA group were enumerated (compounds are racemic or *meso* and included diastereomers where relevant, see Supporting Information for details). This was augmented with a synthetically accessible tropane building block **1f** to give a total of 27 theoretical 3-D building blocks that fitted within our design criteria (i)−(iii). Then, using pyrimidine as a plausible fragment hit (5-bromopyrimidine is a FragLite[31,32]), virtual elaboration on all 27 scaffolds was carried out in conjunction with *N*-capping with methanesulfonyl, acetyl, methyl, and phenyl groups. This gave 112 virtual lead-like compounds (effectively elaborated fragments, examples shown from the nine building blocks, **2a-i**) whose lowest energy conformations were determined using RDKit, an open-source cheminformatics platform. For bifunctional scaffolds, such as those present in the enumerated 112 lead-like compounds, the vectors n_1 and n_2 can be defined by two geometric parameters: the distance through space, r, between the variation points C1 (green atom) and N2 (orange atom) and the dihedral angle, θ, between the two planes defined by the vectors n_1, C1−N2 and n_2 (defined by the red, orange, green, and blue atoms). The parameters r and θ are then readily obtained from the atomic coordinates of the lowest energy conformers of the virtual compounds and allow the construction of a plot of r vs θ.[41] Figure 1D shows an exit vector plot of r vs θ for the 112 lead-like compounds derived from the 27 theoretical 3-D building blocks. Points shown in red correspond to the exit vectors for lead-like compounds **2a-i** (derived from the nine 3-D building blocks **1a-i**) and those in blue are derived from the remaining 18 theoretical 3-D building blocks. The combined plot of red and blue points shows that a wide range of dihedral angles (θ) and spacings (r) is available from the 27 scaffolds. From this plot, we selected 3-D building blocks based on their anticipated ease of synthesis and the fact that they provided a range of distinct 3-D vectors. This ultimately led to the selection of nine 3-D building blocks **1a-i**.

In this paper, we set out the design principles underpinning our modular synthetic platform that enables the straightforward elaboration of typically 2-D fragment hits into 3-D lead-like compounds for use in FBDD. The approach is illustrated with nine bifunctional 3-D building blocks **1a-i** (Figure 1C), whose multigram-scale synthesis is demonstrated. In particular, we present 65 Suzuki-Miyaura cross-coupling reactions between building blocks **1a-i** and medicinally relevant aryl bromides, including a selection of FragLites.[31,32] Several of these cross-coupled arylated products are, after Boc group removal, *N*-functionalized to deliver 32 3-D lead-like compounds. Finally, having validated the synthetic elements of our approach, the synthetic platform is deployed in, and showcased with, the development of a novel and selective Janus kinase 3 (JAK3) inhibitor. Herein, we present our results.

https://doi.org/10.1021/jacs.5c08786
J. Am. Chem. Soc. XXXX, XXX, XXX−XXX

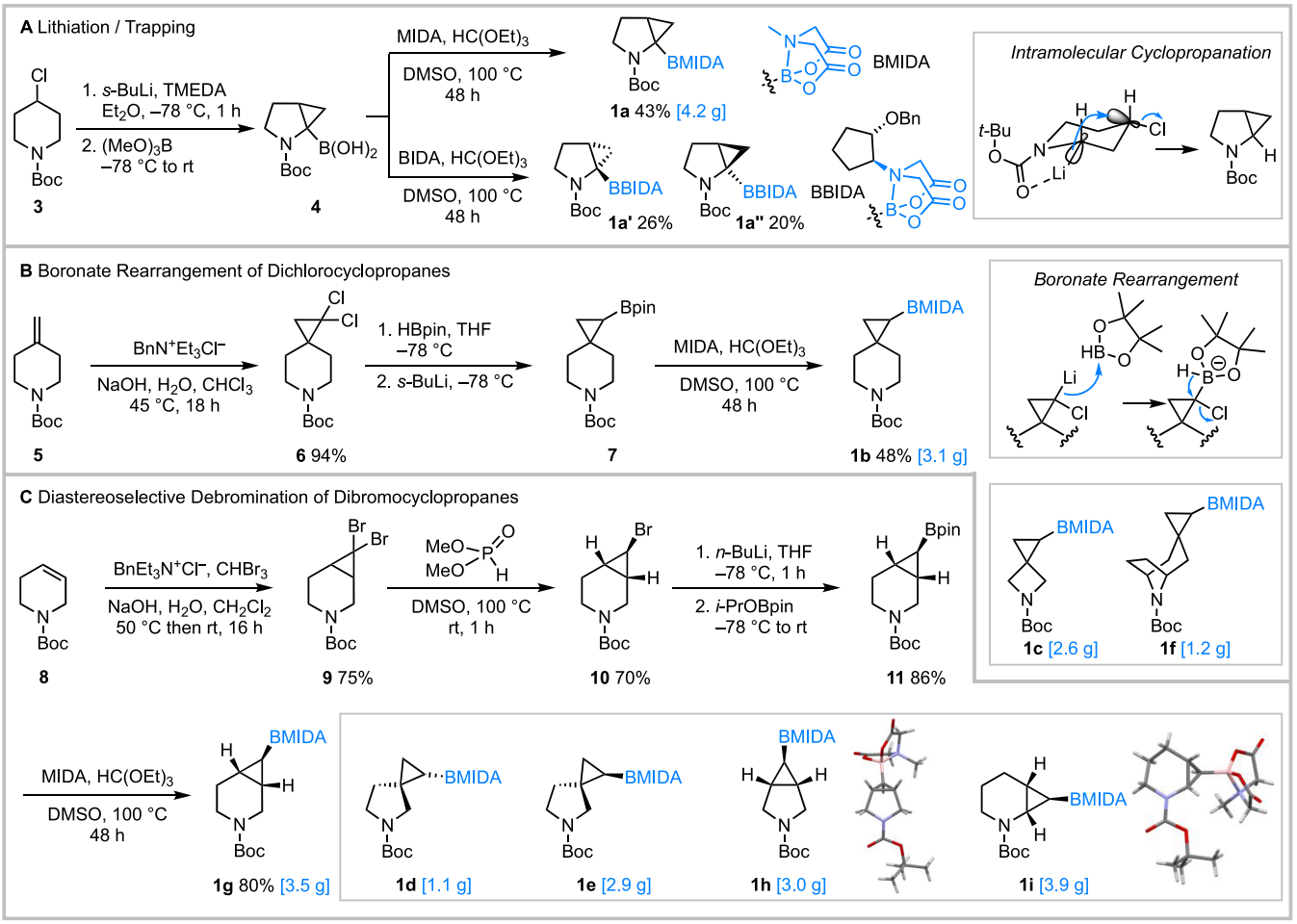

Figure 2. Synthesis of the *N*-Boc MIDA boronate building blocks. (A) Bespoke lithiation/trapping route. (B) Boronate rearrangement of dichlorocyclopropanes. (C) Diastereoselective debromination of dibromocyclopropanes.

RESULTS AND DISCUSSION

Synthesis of 3-D Building Blocks. The different strategies employed for the gram-scale synthesis of each of the nine fused and spirocyclic bifunctional 3-D building blocks **1a-i** are summarized in Figure 2. Fused 2,3-pyrrolidine cyclopropane BMIDA building block **1a** was synthesized via the lithiation−trapping of 4-chloropiperidine **3** using a bespoke synthetic approach.[43,44] Treatment of **3** with *s*-BuLi and TMEDA at −78 °C resulted in α-lithiation, followed by intramolecular cyclopropanation to generate the azabicyclo[3.1.0]hexane ring system (Figure 2A, insert). A second α-lithiation event and subsequent trapping with trimethyl borate gave boronic acid **4**. Finally, conversion into the MIDA boronate using *N*-methyl-iminodiacetic acid (MIDA) and triethylorthoformate in DMSO at 100 °C gave the 3-D building block **1a** (4.2 g prepared in one batch) in 43% yield from **3** (Figure 2A). Use of *N*-2-benzyloxycyclopentyl-iminodiacetic acid (BIDA), an enantiopure chiral MIDA equivalent developed by Burke,[45−47] allowed isolation of enantiomerically pure building blocks. In this exemplar case, condensation of **4** with enantiopure BIDA gave separable diastereomeric 3-D building blocks **1a'** and **1a''** in 26% and 20% yield, respectively (Figure 2A). The configuration of **1a'** and **1a''** was determined by conversion of **1a'** into a cross-coupled product of known configuration (vide infra).

For the synthesis of three spirocyclic 3-D building blocks **1b**, **1c**, and **1f**, a general strategy based on a boronate rearrangement of an intermediate derived from *gem*-dichlorocyclopropanes was developed (Figure 2B). As an example of this synthetic approach, dichlorocyclopropanation of exocyclic alkene-containing *N*-Boc piperidine **5** gave spirocyclic *gem*-dichlorocyclopropane **6** in 94% yield. Treatment of a mixture of **6** and pinacolborane with *s*-BuLi at −78 °C in THF for 30 min gave cyclopropyl pinacol boronate **7**. The reaction presumably proceeds via lithium−halogen exchange and trapping with HBpin followed by 1,2-hydride migration (Figure 2B, insert).[48,49] Conversion of crude pinacol boronate **7** into the corresponding MIDA boronate gave the 3-D building block **1b** (3.1 g prepared in one batch) in 48% yield from **6**. This synthetic approach also enabled the preparation of 2.6 g of spiro-fused cyclopropyl azetidine **1c** and 1.2 g of cyclopropyl tropane **1f** (Figure 2B, insert). Tropane-based 3-D building block **1f** was produced as a single diastereomer as a result of a highly diastereoselective dichlorocyclopropanation reaction, with the dichlorocarbene added opposite to the tropane bridge.

A second general strategy was also developed and was used to access fused 3-D building blocks **1d-1e** and **1g−1i**. For fused 3-D building blocks **1g**, **1h**, and **1i**, an under-developed *exo*-selective diastereoselective debromination[50] of accessible *gem*-dibromocyclopropanes followed by lithium−halogen exchange and *i*-PrOBpin trapping was utilized. The synthesis

https://doi.org/10.1021/jacs.5c08786
J. Am. Chem. Soc. XXXX, XXX, XXX−XXX

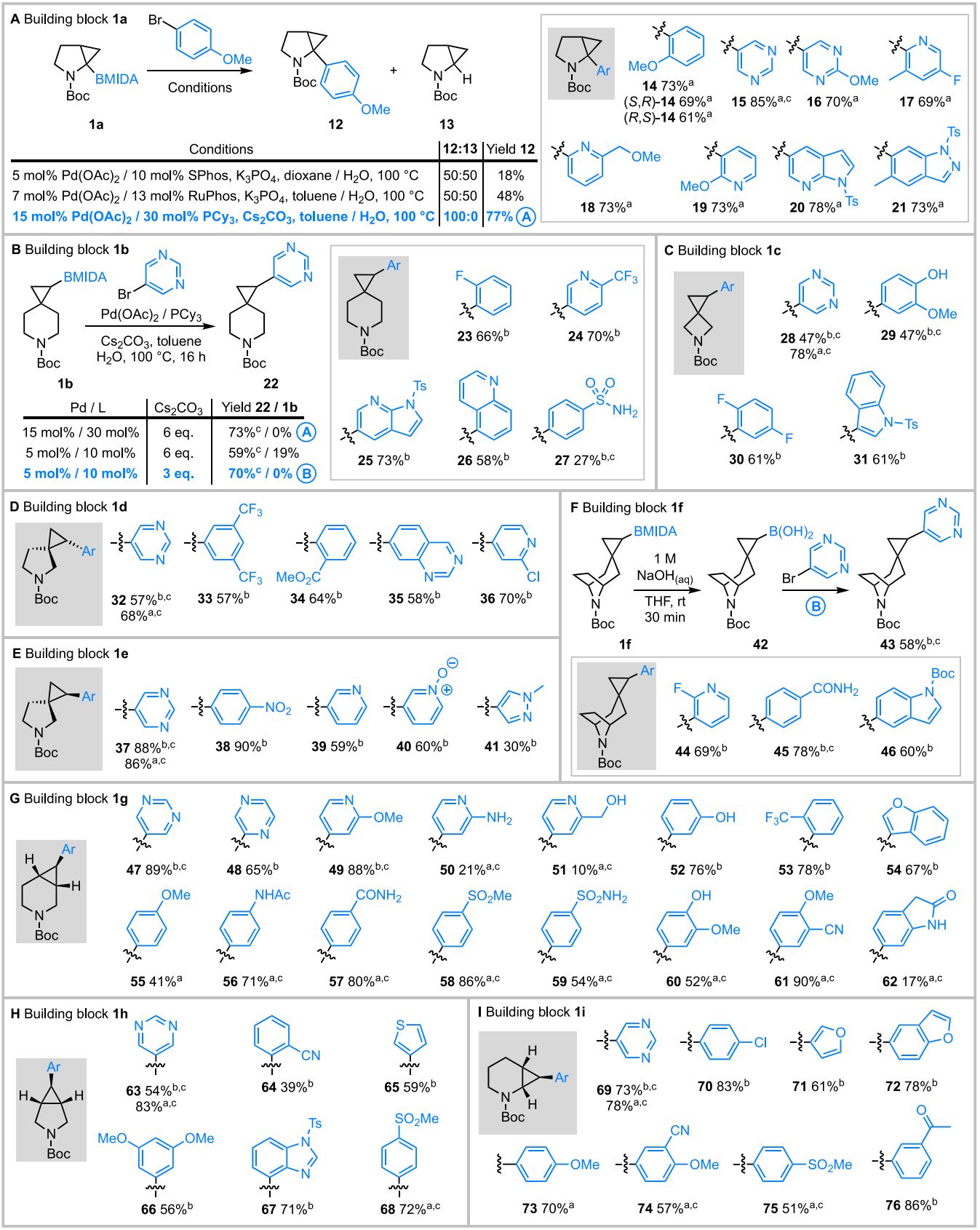

Figure 3. Optimization and scope of the Suzuki-Miyaura cross-coupling of *N*-Boc MIDA boronate building blocks **1a-i**. (A) **1a**. (B) **1b**. (C) **1c**. (D) **1d**. (E) **1e**. (F) **1f**. (G) **1g**. (H) **1h**. (I) **1i**. [a]Using conditions A: 15 mol% $Pd(OAc)_2$, 30 mol% PCy_3, Cs_2CO_3 (6 eq.), ArBr (1.4 eq.), toluene/H_2O, 100 °C, 18 h. [b]Using conditions B: 5 mol% $Pd(OAc)_2$,10 mol% PCy_3, Cs_2CO_3 (3eq.), ArBr (1.4 eq.), toluene/H_2O, 100 °C, 18 h. [c]ArBr is a FragLite.

https://doi.org/10.1021/jacs.5c08786
J. Am. Chem. Soc. XXXX, XXX, XXX−XXX

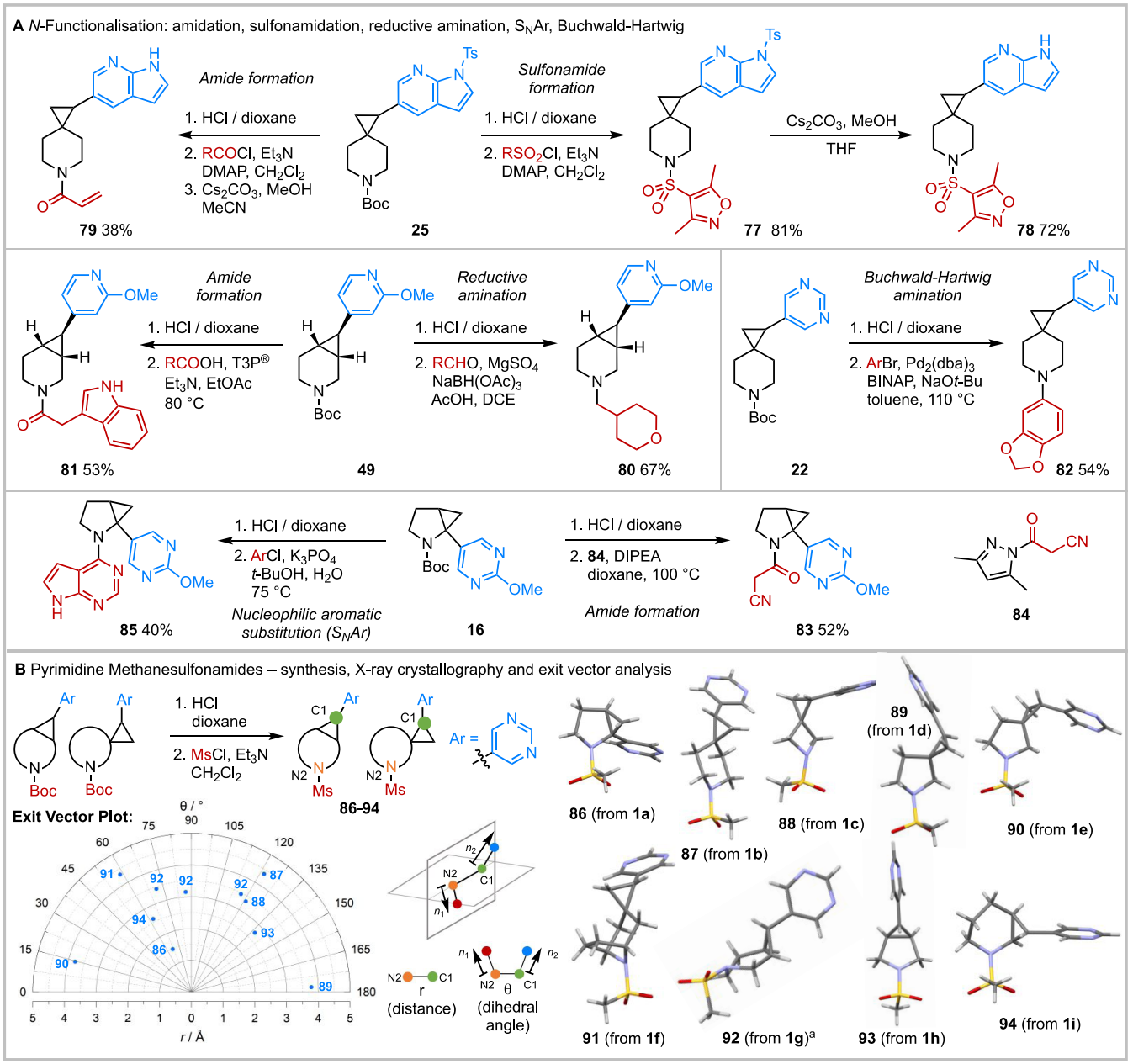

Figure 4. Exemplar diversification of aryl cyclopropanes with medicinally relevant *N*-capping groups and exit vector plot for pyrimidine sulfonamides **86**–**94**. (A) *N*-functionalization. (B) Synthesis, X-ray crystallography, and exit vector plot for **86**–**94** (where applicable, only one enantiomeric series for each compound is displayed on the exit vector plot). [a]The X-ray crystal structure of **92** showed three different conformations but only one structure is shown here (Supporting Information for all three structures). The three conformations for **92** are shown on the exit vector plot.

of **1g** via this approach is shown in Figure 2C. Dibromocyclopropanation of *N*-Boc tetrahydropyridine **8** with NaOH and $CHBr_3$ in CH_2Cl_2–water in the presence of a phase transfer catalyst ($BnEt_3N^+Cl^-$)[51] gave *gem*-dibromocyclopropane **9** in 75% yield. Monodebromination was achieved by treating **9** with dimethylphosphite and KO*t*-Bu in DMSO at 100 °C, a procedure reported by Meijs and Doyle in 1985.[50] This gave *exo*-monobromocyclopropane **10** in 70% yield (configuration assigned from the typical ^3J values for *cis* and *trans* couplings in cyclopropanes[52]), with the stereoselectivity proposed to arise from protonation of a monobromocyclopropane carbanion intermediate to place the bromide in the less sterically hindered *exo* position.[50] Next, pinacol boronate **11** (86% yield) was formed via the stereospecific retentive lithium–halogen exchange of **10** using *n*-BuLi and trapping with *i*-PrOBpin. Treatment of **11** with MIDA gave 3-D building block **1g** (3.5 g prepared in one batch, configuration assigned from ^3J values) in 80% yield. In a similar way, fused 3-D building blocks **1h** (3.0 g) and **1i** (3.9 g) were prepared, and the configuration of each was assigned using X-ray crystallography.[53] The same route was also used to synthesize diastereomeric spirocyclic pyrrolidines **1d** (1.1 g) and **1e** (2.9 g). In this case, due to similar steric hindrance on each side of the cyclopropane ring, the monodebromination reaction lacked diastereoselectivity: a 55:45 mixture of diastereomeric monobromides was formed. The configurations of **1d** and **1e**

https://doi.org/10.1021/jacs.5c08786
J. Am. Chem. Soc. XXXX, XXX, XXX−XXX

were assigned based on the X-ray crystal structure of the monobromocyclopropane that was an intermediate in the synthesis of **1e** (see Supporting Information for full details). To facilitate the use of 3-D building blocks **1a-i**, all nine building blocks are commercially available.

Elaboration of 3-D Building Blocks. With the nine bifunctional 3-D building blocks **1a-i** in hand, the next stage involved demonstrating that both functional groups could be utilized in the planned elaboration methodology. Initial focus was on the development of general conditions for the Suzuki-Miyaura cross-coupling with aryl and heteroaryl bromides (Figure 3). Cross-coupling of 2,3-pyrrolidine cyclopropane BMIDA **1a** with 4-bromoanisole using Burke's conditions[35] (5 mol % $Pd(OAc)_2$/10 mol % SPhos and K_3PO_4 in dioxane/H_2O) gave a 50:50 mixture of aryl cyclopropane **12** and unsubstituted cyclopropane **13** (protodeboronation product), with only an 18% isolated yield of pure **12**. Use of 7 mol % $Pd(OAc)_2$/13 mol % RuPhos and K_2CO_3 in toluene/H_2O at 100 °C[36] also gave a 50:50 mixture of **12** and **13**, but with an improved 48% yield of **12**. In contrast, use of 15 mol % $Pd(OAc)_2$/30 mol % PCy_3 and 6 eq. Cs_2CO_3 in toluene/H_2O at 100 °C (conditions A)[34] gave only **12**, isolated in 77% yield (Figure 3A). Attempts to reduce the catalyst loading for reactions of BMIDA **1a** led to significant formation of **13**, presumably due to protodeboronation of the cyclopropyl boronic acid that is formed in situ. Using conditions A, cross-coupling of BMIDA **1a** with a range of 2-D fragment-like heteroaryl bromides, including pyrimidines, pyridines, *N*-tosyl 7-azaindole, and a *N*-tosyl indazole, gave aryl cyclopropanes **14**-**21** in 69−85% yield (Figure 3A). Access to enantiopure cross-coupled products was demonstrated using 2-bromoanisole; readily separable enantiopure BBIDA diastereomeric building blocks **1a**' and **1a**'' were converted into enantiomeric aryl cyclopropanes (*S*,*R*)-**14** (69%) (known configuration)[44] and (*R*,*S*)-**14** (61%), respectively (Figure 3A).

Conditions A were also applied to the cross-coupling between spiro piperidine BMIDA **1b** and 5-bromopyrimidine, which gave aryl cyclopropane **22** in 73% yield (Figure 3B). In this case, lowering the catalyst loading to 5 mol % $Pd(OAc)_2$/10 mol % PCy_3 was accommodated, with **22** being obtained in 59% yield, together with unhydrolyzed BMIDA **1b** (19%). Reducing the amount of Cs_2CO_3 from 6 eq. to 3 eq. at this lower catalyst loading gave a 70% yield of aryl cyclopropane **22**. The majority of the cross-coupling examples were carried out under these conditions, namely, 5 mol % $Pd(OAc)_2$/10 mol % PCy_3 and 3 eq. Cs_2CO_3 in toluene/H_2O at 100 °C (conditions B). Issues were encountered in the attempted cross-couplings using cyclopropyl tropane BMIDA **1f**, as a low yield (29%, conditions B) of **43** was obtained. This was believed to be due to BMIDA **1f** not being fully soluble in toluene/water. Other solvents were explored without success, and use of the analogous Bpin derivative of **1f** gave **43** in 39% yield. As a result, ex situ hydrolysis of the MIDA boronate group of **1f** to the presumed boronic acid **42** was performed with $NaOH_{(aq)}$ prior to cross-coupling.[47] Then, cross-coupling of crude boronic acid **42** using conditions B gave aryl cyclopropane **43** in 58% yield. Similarly, using this two-step approach, **44**-**46** were obtained in 60−78% yield (Figure 3F).

Using conditions A and B, 3-D building blocks **1a-i** were cross-coupled with a wide range of aryl and heteroaryl bromides, with retention of configuration where relevant, as shown by X-ray crystallography of pyrimidine methanesulfonamides (vide infra, see Figure 4). Figure 3 illustrates 63 examples; yields ranged from 10 to 90%, and most were ≥ 60%. Electron-poor (**23**, **30**, **33**, **38**, **53**, **58**, **64**, **68**, **75**, **76**) and electron-rich (**12**, **14**, **29**, **52**, **55**, **56**, **66**, **73**) aryl bromides were well tolerated, as was a range of heteroaryl groups, including azaindole (**20**, **25**), indazole (**21**), quinoline (**26**), indole (**31**, **46**), quinazoline (**35**), pyrazole (**41**), benzofuran (**54**, **72**), thiophene (**65**), benzimidazole (**67**), and furan (**71**). Given the usefulness of the FragLite screening set in mapping out protein binding sites[31,32] and their challenging functionality for cross-couplings, 11 distinct FragLites were included in our study of scope (examples with FragLites include **15**, **22**, **27**−**29**, **32**, **37**, **43**, **45**, **47**, **49**−**51**, **56**−**62**, **63**, **68**, **69**, **74**−**75**). There were some unsuccessful cross-coupling reactions, and these are presented in the Supporting Information. In addition, potassium trifluoroborate derivatives analogous to cyclopropyl BMIDAs **1b**, **1c**, **1f**, and **1g** were readily prepared and cross-coupled successfully (see Supporting Information for full details). In summary, all nine 3-D building blocks **1a-i** were successfully cross-coupled with 46 different aryl and heteroaryl bromides to generate 63 *N*-Boc aryl cyclopropanes (Figure 3).

Next, to validate that the nine 3-D building blocks **1a-i** would be suitable for fragment elaboration, we explored deprotection and diversification of the amine functionality of a selection of the *N*-Boc aryl cyclopropanes with a range of chemistries and capping groups commonly employed by medicinal chemists (Figure 4A).[26] The Boc group was removed from aryl cyclopropanes **16**, **22**, **25**, and **49** using HCl/dioxane to give crude hydrochloride salts for subsequent reactions. Starting from azaindolyl spiro piperidine **25**, reaction with a sulfonyl chloride gave sulfonamide **77**, and subsequent treatment with Cs_2CO_3/MeOH[54] removed the *N*-tosyl group to give azaindole sulfonamide **78**. In a similar way, **25** was converted into acrylamide **79** (using acryloyl chloride); acrylamides are commonly employed as covalent warheads, and this approach is gaining significant prominence in medicinal chemistry.[55] Methoxy pyridine-containing fused piperidine **49** was derivatized in two different ways: reductive amination delivered *N*-alkyl derivative **80** and amidation using T3P and a carboxylic acid gave amide **81**. Pyrimidinyl spiro piperidine **22** was *N*-arylated using a Buchwald-Hartwig reaction to give *N*-aryl piperidine **82**. Another covalent warhead was added to methoxypyrimidinyl-fused pyrrolidine **16**, via amidation with acyl pyrazole **84**, to give amide **83**. Alternatively, starting from **22**, a S_NAr reaction with 4-chloro-7H-pyrrolo[2,3-*d*]pyrimidine led to *N*-aryl pyrrolidine **85**.

A key design feature of 3-D building blocks **1a-i** was that they would access a range of 3-D vectors and 3-D chemical space. To show this, each of the building blocks **1a-i** was cross-coupled with 5-bromopyrimidine (see Figure 3) and subsequently converted into the corresponding methanesulfonamides **86**−**94** (Figure 4B). As anticipated, sulfonamides **86**−**94** were crystalline, and each was analyzed by X-ray crystallography. The X-ray crystal structures and the exit vector plot of r (distance) vs θ (dihedral angle)[41] for sulfonamides **86**−**94** are shown in Figure 4B. For fused piperidine **92**, three conformations (only one shown) were found in the asymmetric unit in the X-ray crystal structure, and all three conformations are presented on the exit vector plot of r vs θ. Of note, the r vs θ plot shows that sulfonamides **86**−**94**, derived from building blocks **1a-i**, respectively, cover a wide and varied range of chemical space, with distances between variation points (r) of 1.5−4.4 Å and a range of spatial orientations of the diversification groups (θ).

https://doi.org/10.1021/jacs.5c08786
J. Am. Chem. Soc. XXXX, XXX, XXX−XXX

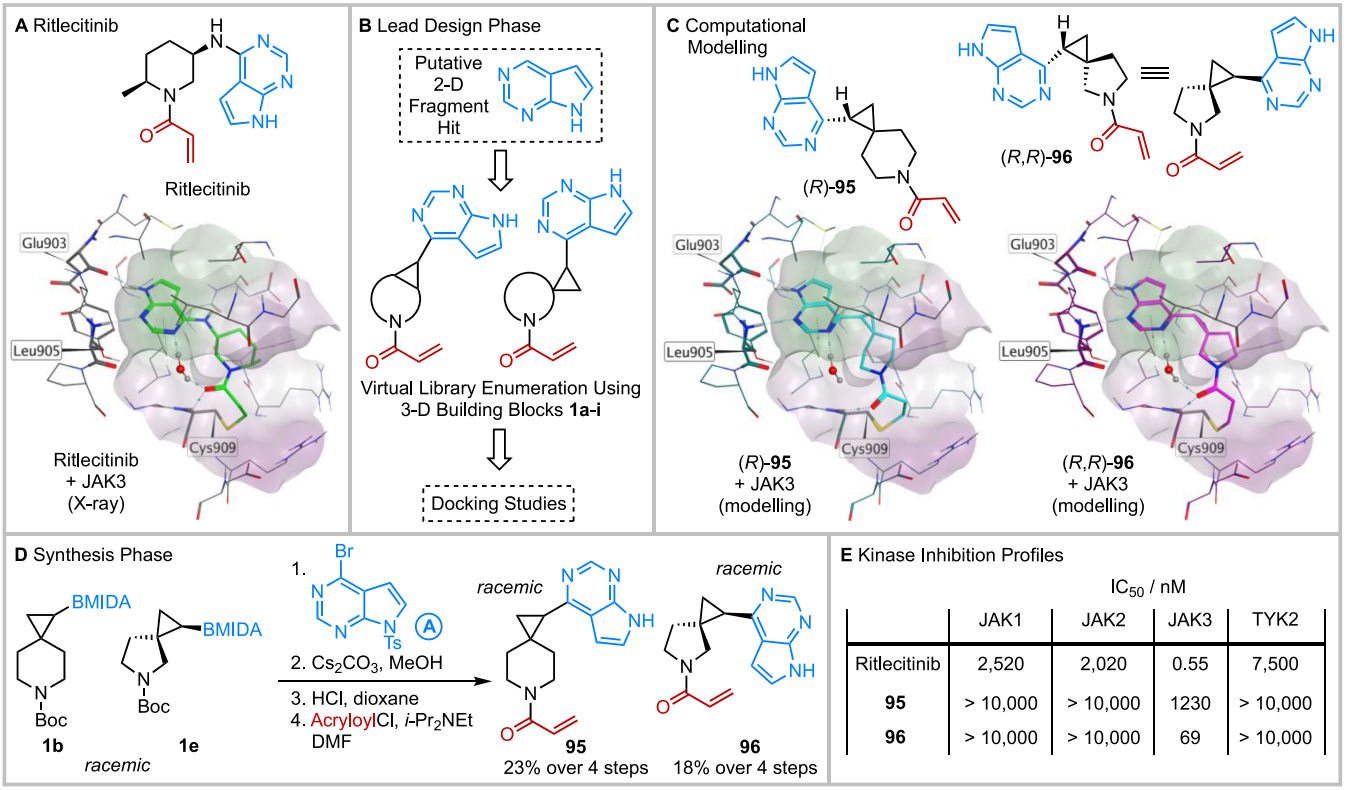

Figure 5. Design and synthesis of a JAK3 selective inhibitor. (A) Cocrystal X-ray structure of ritlecitinib and JAK3. (B) Lead design phase. (C) Computational modeling of (*R*)-**95** and (*R,R*)-**96** and JAK3. (D) Synthesis of racemic **95** and **96**. (E) Kinase inhibition profiles of ritlecitinib, **95**, and **96** against JAK1, JAK2, JAK3, and TYK2 (see Supporting Information for details on the concentrations of reagents used in the assay).

For the synthesis of 3-D lead-like compounds from putative 2-D fragments and 3-D building blocks **1a-i**, the 16 examples of *N*-functionalization shown in Figure 4A,B were supplemented by 16 further examples (see Supporting Information) to give 32 3-D lead-like compounds. The lead-like nature of the compounds was confirmed by the analysis of their calculated molecular properties. Under Churcher's definition,[11] compounds occupy lead-like chemical space if they have suitable lipophilicity ($-1 < \text{clogP} < 3$) and molecular weight (200−350 Da), with a low degree of aromatic character. The 32 exemplar compounds have a mean clogP of 0.46, a mean MW of 266, and a mean fraction of sp^3 hybridized carbon atoms (Fsp^3)[10] of 0.56, and thus comfortably occupy lead-like space (29 of the 32 compounds satisfy these lead-like criteria; values for each lead-like compound are provided in the Supporting Information). In addition, 12 of the lead-like compounds (**78**, **81**, **82**, and **86**−**94**) were subjected to AstraZeneca's drug metabolism and pharmacokinetics (DMPK) Wave1 analysis.[56] This provides information on lipophilicity (measured logD), aqueous solubility, and metabolic stability in human liver microsomes (HLM) and rat hepatocytes (RH) (see Supporting Information for full details). For the 12 compounds, logD ranged from −0.4 to 3.6, and all exhibited suitable aqueous solubility (49.0 to >981 μM). Ten of the 12 compounds (**82** and all sulfonamides **86**−**94**) showed good metabolic stability in both assays; compounds **78** and **81**, which had the highest logD values, have benzylic positions and/or an electron-rich indole ring which likely accounts for their lower metabolic stability. This also shows that the metabolic profile will be dependent on the overall properties of the molecules designed using 3-D building blocks **1a-i** and that there are no intrinsic liabilities with the cyclopropyl building block scaffolds.

Design and Synthesis of a Selective JAK3 Inhibitor. Having demonstrated the synthesis phase (see Figure 1B) of the fragment elaboration synthetic platform, the final element was to showcase our approach with the design and synthesis of a 3-D lead compound using the lead design phase (see Figure 1A). For this, the development of a Janus kinase (JAK) inhibitor related to Ritlecitinib was targeted. The Janus kinases are a family of nonreceptor tyrosine kinases (TYK), which control cytokine signaling, and are common targets for the modulation of autoimmune, autoinflammatory, and allergic diseases. Ritlecitinib (PF-06651600) (Figure 5A), a covalent inhibitor of JAK3 that shows selectivity over the other JAK isoforms JAK1, JAK2, and TYK2,[57] was approved in 2023 for the treatment of alopecia areata. The X-ray crystal structure of the JAK3 covalent adduct formed from Cys909 reacting with the acrylamide of Ritlecitinib is shown in Figure 5A. In addition to this covalent bond, the pyrrolopyrimidine was hydrogen bonded with Glu903 and Leu905 in JAK3. In addition, a key conformational activation of the acrylamide was identified from water-linked hydrogen bonds from the pyrimidine to the carbonyl group of the acrylamide.

For our fragment elaboration docking studies, we first imagined that the pyrrolopyrimidine was an initial 2-D fragment hit that had bound in the kinase hinge region of JAK3 in the same pose as Ritlecitinib. Nine potential lead-like compounds were then virtually enumerated by combining the pyrrolopyrimidine (from the 4-position) with each of the nine 3-D building blocks **1a-i** which were *N*-functionalized with an acrylamide (Figure 5B). Computational modeling of each

https://doi.org/10.1021/jacs.5c08786
J. Am. Chem. Soc. XXXX, XXX, XXX−XXX

enantiomer of these lead-like compounds (except for that derived from **1h** which is meso) was carried out by docking the pyrrolopyrimidine to Glu903 and Leu905 with and without a covalent bond to the acrylamide. The poses with the lowest docking scores/energies and similar conformational features to the Ritlecitinib−JAK3 complex were identified (see Supporting Information for details). The modeled complexes for **95** and **96** bound to JAK3 are shown in Figure 5C. From this analysis, acrylamides **95** and **96** were targeted for synthesis. Of note, **95** and **96** (derived from 3-D building blocks **1b** and **1e**) were readily synthesized since the synthetic methodology to do so (Suzuki-Miyaura cross-coupling, tosyl and Boc group removal and acrylamide formation, Figure 5D) was already established, thus highlighting that building blocks **1a-i** are synthetically enabled. Acrylamides **95** and **96** were evaluated in a biochemical kinase inhibition assay, screening against JAK1/2/3 and TYK2 at a 1 h time point.[58] Both **95** and **96** were selective for JAK3, with no inhibition (>10,000 nM) of JAK1, JAK2, or TYK2 (Figure 5E). Pleasingly, **96** was a potent inhibitor of JAK3, with IC_{50} = 69 nM, with **95** being less potent, and with IC_{50} = 1.23 μM (see Supporting Information). Although **96** was ∼10-fold less active than Ritlecitinib (IC_{50} = 0.55 nM under the same assay conditions, where the ATP concentration is close to K_m), **96** has a better selectivity profile against JAK1, JAK2, and TYK2 compared to Ritlecitinib (Figure 5E). In addition, racemic **95** and **96** were evaluated, whereas Ritlecitinib is a single enantiomer. The better inhibition results for **96** compared to **95** may be due to the fully formed water-linked hydrogen bonds from the pyrimidine to the carbonyl group of the acrylamide in the computational modeling of the docking pose (Figure 5C). Of note, the glutathione (GSH) reactivity of both **96** and Ritlecitinib were similar: $t_{1/2}$ for **96** is 1254 min and $t_{1/2}$ for Ritlecitinib is 2020 min in a comparative assay[59] (see Supporting Information). Thus, using both the lead design and synthesis phases, we have demonstrated elaboration of the putative 2-D fragment hit, pyrrolopyrimidine, using 3-D building block **1e** (identified from the computational docking studies) into 3-D lead-like compound **96** which is a selective inhibitor of JAK3, with IC_{50} = 69 nM. Our approach is complementary to that reported by Reymond et al. for the discovery of a JAK1 selective inhibitor and a JAK3 selective inhibitor, each based on a novel triquinazine scaffold.[60]

CONCLUSIONS

In conclusion, we have developed a modular synthetic platform for the systematic and programmable elaboration of 2-D fragment hits into 3-D lead-like compounds for use in FBDD. The design and gram-scale synthesis of nine bifunctional 3-D building blocks **1a-i**, together with a wide range of Suzuki-Miyaura cross-coupling reactions (65 examples) and *N*-functionalizations (32 lead-like compounds), are presented. Crucially, each of the 3-D building blocks **1a-i** accesses a distinct 3-D exit vector, as shown both by analysis of the lowest energy conformations of potential lead-like molecules using RDKit (Figure 1D) and by X-ray crystallography of methanesulfonamides (Figure 4B). The design and synthesis of a selective inhibitor of JAK3 with IC_{50} = 69 nM showcased the synthetic platform, with the rapid generation of lead-like compounds from an initial 2-D fragment hit. In this way, our methodology is a step toward addressing the call to arms from industry by providing the synthetic "elaboration of fragments in three dimensions from many different growth points/vectors using methodology that is worked out prior to fragment screening."[14] Of note, 3-D building blocks **1a-i** are commercially available. Future efforts will be directed toward the development of additional bifunctional 3-D building blocks that provide entry into 3-D exit vectors that are not covered by 3-D building blocks **1a-i**. In this way, the synthetic platform will be expanded to provide a comprehensive coverage of 3-D vector and chemical space for use in FBDD.

ASSOCIATED CONTENT

Supporting Information

The Supporting Information is available free of charge at https://pubs.acs.org/doi/10.1021/jacs.5c08786.

Experimental procedures and characterization data; exit vector analysis; lead-like analysis; DMPK analysis; and molecular modeling and inhibition studies (PDF)

Accession Codes

Deposition Numbers 2219554−2219566 contain the supplementary crystallographic data for this paper. These data can be obtained free of charge via the joint Cambridge Crystallographic Data Centre (CCDC) and Fachinformationszentrum Karlsruhe Access Structures service.

AUTHOR INFORMATION

Corresponding Author

Peter O'Brien − *Department of Chemistry, University of York, York YO10 5DD, U.K.*; orcid.org/0000-0002-9966-1962; Email: peter.obrien@york.ac.uk

Authors

Andres R. Gomez-Angel − *Department of Chemistry, University of York, York YO10 5DD, U.K.*

Hanna F. Klein − *Department of Chemistry, University of York, York YO10 5DD, U.K.*

Stephen Y. Yao − *Department of Chemistry, University of York, York YO10 5DD, U.K.*

James R. Donald − *Department of Chemistry, University of York, York YO10 5DD, U.K.*

James D. Firth − *Department of Chemistry, University of York, York YO10 5DD, U.K.*

Rebecca Appiani − *Department of Chemistry, University of York, York YO10 5DD, U.K.*

Cameron J. Palmer − *Department of Chemistry, University of York, York YO10 5DD, U.K.*

Joshua Lincoln − *Department of Chemistry, University of York, York YO10 5DD, U.K.*

Simon C. C. Lucas − *Hit Discovery, Discovery Sciences, R&D, AstraZeneca, Cambridge CB2 0AA, U.K.*; orcid.org/0000-0002-9172-8739

Lucia Fusani − *Hit Discovery, Discovery Sciences, R&D, AstraZeneca, Cambridge CB2 0AA, U.K.*

R. Ian Storer − *Hit Discovery, Discovery Sciences, R&D, AstraZeneca, Cambridge CB2 0AA, U.K.*

Complete contact information is available at: https://pubs.acs.org/10.1021/jacs.5c08786

Author Contributions

[§]A.R.G.-A., H.F.K. and S.Y.Y. contributed equally to this work. The manuscript was written through contributions of all authors. All authors have given approval to the final version of the manuscript.

https://doi.org/10.1021/jacs.5c08786
J. Am. Chem. Soc. XXXX, XXX, XXX−XXX

Funding

This project was funded by The Royal Society (Industry Fellowship with AstraZeneca, INF\R1\191028, POB), the EU (Horizon 2020 program, Marie Skłodowska-Curie grant agreement No. 675899, FRAGNET), the EPSRC (EP/V048139/1, JDF; Impact Accelerator Account (IAA), JRD), and the Higher Education Innovation Fund (HEIF) (JRD).

Notes

The authors declare the following competing financial interest(s): The University of York, POB, HFK, SYY and JRD receive royalties from the sale of building blocks **1a-i**. SCCL, LF and RIS are employees of AstraZeneca.

■ ACKNOWLEDGMENTS

This paper is dedicated to the memory of Dr. Stuart Warren, an inspiring educator, writer, and mentor. We gratefully acknowledge support from the University of York Wild Fund (A.R.G.-A. and S.Y.Y.). Redbrick Molecular and Key Organics are acknowledged for their interest in this project. We thank Dr. Adrian C. Whitwood for X-ray crystallography.

■ ABBREVIATIONS

FBDD, fragment-based drug discovery; MW, molecular weight; 3-D, 3-dimensional; 2-D, 2-dimensional; Boc, *tert*-butoxy carbonyl; S_NAr, nucleophilic aromatic substitution; MIDA, *N*-methyliminodiacetic acid; BMIDA, *N*-methyliminodiacetic acid boronate; JAK3, Janus kinase 3; TMEDA, *N,N,N′,N′*-tetramethylethylene-diamine; DMSO, dimethyl sulfoxide; BIDA, *N*-2-benzyloxycyclopentyl-iminodiacetic acid; pin, piacolate; SPhos, 2-dicyclohexylphosphino-2′,6′-dimethoxybiphenyl; RuPhos, 2-dicyclohexylphosphino-2′,6′-diisopropoxybiphenyl; DMPK, drug metabolism and pharmacokinetics; TYK, nonreceptor tyrosine kinase

■ REFERENCES

(1) Murray, C. W.; Rees, D. C. The rise of fragment-based drug discovery. *Nat. Chem.* **2009**, *1*, 187−192.

(2) Congreve, M.; Chessari, G.; Tisi, D.; Woodhead, A. J. Recent Developments in Fragment-Based Drug Discovery. *J. Med. Chem.* **2008**, *51*, 3661−3680.

(3) Keserű, G. M.; Erlanson, D. A.; Ferenczy, G. G.; Hann, M. M.; Murray, C. W.; Pickett, S. D. Design Principles for Fragment Libraries: Maximizing the Value of Learnings from Pharma Fragment-Based Drug Discovery (FBDD) Programs for Use in Academia. *J. Med. Chem.* **2016**, *59*, 8189−8206.

(4) Erlanson, D. A.; Fesik, S. W.; Hubbard, R. E.; Jahnke, W.; Jhoti, H. Twenty years on: the impact of fragments on drug discovery. *Nat. Rev. Drug Discovery* **2016**, *15*, 605−619.

(5) Lamoree, B.; Hubbard, Roderick E. Current perspectives in fragment-based lead discovery (FBLD). *Essays Biochem.* **2017**, *61*, 453−464.

(6) Erlanson, D. A. Fragments in the clinic 2024 http://practicalfragments.blogspot.com/2024/02/fragments-in-clinic-2024-edition.html (accessed May 1, 2025).

(7) Xu, W.; Congbao, K. Fragment-Based Drug Design: From Then until Now, and Toward the Future. *J. Med. Chem.* **2025**, *68*, 5000−5004.

(8) Congreve, M.; Carr, R.; Murray, C.; Jhoti, H. A 'Rule of Three' for fragment-based lead discovery? *Drug Discovery Today* **2003**, *8*, 876−877.

(9) Hall, R. J.; Mortenson, P. N.; Murray, C. W. Efficient exploration of chemical space by fragment-based screening. *Prog. Biophys. Mol. Bio.* **2014**, *116*, 82−91.

(10) Lovering, F.; Bikker, J.; Humblet, C. Escape from Flatland: Increasing Saturation as an Approach to Improving Clinical Success. *J. Med. Chem.* **2009**, *52*, 6752−6756.

(11) Nadin, A.; Hattotuwagama, C.; Churcher, I. Lead-Oriented Synthesis: A New Opportunity for Synthetic Chemistry. *Angew. Chem., Int. Ed.* **2012**, *51*, 1114−1122.

(12) Brown, D. G.; Boström, J. Analysis of Past and Present Synthetic Methodologies on Medicinal Chemistry: Where Have All the New Reactions Gone? *J. Med. Chem.* **2016**, *59*, 4443−4458.

(13) Boström, J.; Brown, D. G.; Young, R. J.; Keserü, G. M. Expanding the medicinal chemistry synthetic toolbox. *Nat. Rev. Drug Discovery* **2018**, *17*, 709−727.

(14) Murray, C. W.; Rees, D. C. Opportunity Knocks: Organic Chemistry for Fragment-Based Drug Discovery (FBDD). *Angew. Chem., Int. Ed.* **2016**, *55*, 488−492.

(15) Blakemore, D. C.; Castro, L.; Churcher, I.; Rees, D. C.; Thomas, A. W.; Wilson, D. M.; Wood, A. Organic synthesis provides opportunities to transform drug discovery. *Nat. Chem.* **2018**, *10*, 383−394.

(16) Palmer, N.; Peakman, T. M.; Norton, D.; Rees, D. C. Design and synthesis of dihydroisoquinolones for fragment-based drug discovery (FBDD). *Org. Biomol. Chem.* **2016**, *14*, 1599−1610.

(17) Downes, T. D.; Jones, S. P.; Klein, H. F.; Wheldon, M. C.; Atobe, M.; Bond, P. S.; Firth, J. D.; Chan, N. S.; Waddelove, L.; Hubbard, R. E.; Blakemore, D. C.; De Fusco, C.; Roughley, S. D.; Vidler, L. R.; Whatton, M. A.; Woolford, A. J.-A.; Wrigley, G. L.; O'Brien, P. Design and Synthesis of 56 Shape-Diverse 3D Fragments. *Chem. - Eur. J.* **2020**, *26*, 8969−8975.

(18) Jones, S. P.; Firth, J. D.; Wheldon, M. C.; Atobe, M.; Hubbard, R. E.; Blakemore, D. C.; De Fusco, C.; Lucas, S. C. C.; Roughley, S. D.; Vidler, L. R.; Whatton, M. A.; Woolford, A. J.-A.; Wrigley, G. L.; O'Brien, P. Exploration of piperidine 3D fragment chemical space: synthesis and 3D shape analysis of fragments derived from 20 regio- and diastereoisomers of methyl substituted pipecolinates. *RSC Med. Chem.* **2022**, *13*, 1614−1620.

(19) Hamilton, D. J.; Dekker, T.; Klein, H. F.; Janssen, G. V.; Wijtmans, M.; O'Brien, P.; de Esch, I. J. P. Escape from planarity in fragment-based drug discovery: A physicochemical and 3D property analysis of synthetic 3D fragment libraries. *Drug Discovery Today: Technol.* **2020**, *38*, 77−90.

(20) Klein, H. F.; Hamilton, D. J.; de Esch, I. J. P.; Wijtmans, M.; O'Brien, P. Escape from planarity in fragment-based drug discovery: A synthetic strategy analysis of synthetic 3D fragment libraries. *Drug Discovery Today* **2022**, *27*, 2484−2496.

(21) Chessari, G.; Grainger, R.; Holvey, R. S.; Ludlow, R. F.; Mortenson, P. N.; Rees, D. C. C−H functionalisation tolerant to polar groups could transform fragment-based drug discovery (FBDD). *Chem. Sci.* **2021**, *12*, 11976−11985.

(22) Grainger, R.; Heightman, T. D.; Ley, S. V.; Lima, F.; Johnson, C. N. Enabling synthesis in fragment-based drug discovery by reactivity mapping: photoredox-mediated cross-dehydrogenative heteroarylation of cyclic amines. *Chem. Sci.* **2019**, *10*, 2264−2271.

(23) Trindade, A. F.; Faulkner, E. L.; Leach, A. G.; Nelson, A.; Marsden, S. P. Fragment-oriented synthesis: *β*-elaboration of cyclic amine fragments using enecarbamates as platform intermediates. *Chem. Commun.* **2020**, *56*, 8802−8805.

(24) Caplin, M. J.; Foley, D. J. Emergent synthetic methods for the modular advancement of sp^3-rich fragments. *Chem. Sci.* **2021**, *12*, 4646−4660.

(25) St Denis, J. D.; Hall, R. J.; Murray, C. W.; Heightman, T. D.; Rees, D. C. Fragment-based drug discovery: opportunities for organic synthesis. *RSC Med. Chem.* **2021**, *12*, 321−329.

(26) Roughley, S. D.; Jordan, A. M. The Medicinal Chemist's Toolbox: An Analysis of Reactions Used in the Pursuit of Drug Candidates. *J. Med. Chem.* **2011**, *54*, 3451−3479.

(27) Bauer, M. R.; Di Fruscia, P.; Lucas, S. C. C.; Michaelides, I. N.; Nelson, J. E.; Storer, R. I.; Whitehurst, B. C. Put a ring on it: application of small aliphatic rings in medicinal chemistry. *RSC Med. Chem.* **2021**, *12*, 448−471.

https://doi.org/10.1021/jacs.5c08786
J. Am. Chem. Soc. XXXX, XXX, XXX−XXX

(28) Talele, T. T. The "Cyclopropyl Fragment" is a Versatile Player that Frequently Appears in Preclinical/Clinical Drug Molecules. *J. Med. Chem.* **2016**, *59*, 8712−8756.
(29) Li, J.; Ballmer, S. G.; Gillis, E. P.; Fujii, S.; Schmidt, M. J.; Palazzolo, A. M. E.; Lehmann, J. W.; Morehouse, G. F.; Burke, M. D. Synthesis of many different types of organic small molecules using one automated process. *Science* **2015**, *347*, 1221−1226.
(30) Goldberg, F. W.; Kettle, J. G.; Kogej, T.; Perry, M. W. D.; Tomkinson, N. P. Designing novel building blocks is an overlooked strategy to improve compound quality. *Drug Discovery Today* **2015**, *20*, 11−17.
(31) Wood, D. J.; Lopez-Fernandez, J. D.; Knight, L. E.; Al-Khawaldeh, I.; Gai, C.; Lin, S.; Martin, M. P.; Miller, D. C.; Cano, C.; Endicott, J. A.; Hardcastle, I. R.; Noble, M. E. M.; Waring, M. J. FragLites—Minimal, Halogenated Fragments Displaying Pharmacophore Doublets. An Efficient Approach to Druggability Assessment and Hit Generation. *J. Med. Chem.* **2019**, *62*, 3741−3752.
(32) Davison, G.; Martin, M. P.; Turberville, S.; Dormen, S.; Heath, R.; Heptinstall, A. B.; Lawson, M.; Miller, D. C.; Ng, Y. M.; Sanderson, J. N.; Hope, I.; Wood, D. J.; Cano, C.; Endicott, J. A.; Hardcastle, I. R.; Noble, M. E. M.; Waring, M. J. Mapping Ligand Interactions of Bromodomains BRD4 and ATAD2 with FragLites and PepLites—Halogenated Probes of Druglike and Peptide-like Molecular Interactions. *J. Med. Chem.* **2022**, *65*, 15416−15432.
(33) Singh, V. P.; Singh, H. B.; Butcher, R. J. Synthesis and Glutathione Peroxidase-Like Activities of Isoselenazolines. *Eur. J. Org. Chem.* **2011**, *2011*, 5485−5497.
(34) Singh, R.; Tso, K.; Zhang, J.; Duncton, M. Protein Kinase C Inhibitors And Uses Thereof. US20110130415A1.2011.
(35) Knapp, D. M.; Gillis, E. P.; Burke, M. D. A General Solution for Unstable Boronic Acids: Slow-Release Cross-Coupling from Air-Stable MIDA Boronates. *J. Am. Chem. Soc.* **2009**, *131*, 6961−6963.
(36) Duncton, M. A. J.; Singh, R. Synthesis of trans-2-(Trifluoromethyl)cyclopropanes via Suzuki Reactions with an N-Methyliminodiacetic Acid Boronate. *Org. Lett.* **2013**, *15*, 4284−4287.
(37) Kleban, I.; Radchenko, D. S.; Tymtsunik, A. V.; Shuvakin, S.; Konovets, A. I.; Rassukana, Y.; Grygorenko, O. O. Cyclopropyl boronic derivatives in parallel synthesis of sp3-enriched compound libraries. *Monatsh. Chem.* **2020**, *151*, 953−962.
(38) Gutiérrez-Bonet, Á.; Popov, S.; Emmert, M. H.; Hughes, J. M. E.; Nolting, A. F.; Ruccolo, S.; Wang, Y. Asymmetric Synthesis of Tertiary and Secondary Cyclopropyl Boronates via Cyclopropanation of Enantioenriched Alkenyl Boronic Esters. *Org. Lett.* **2022**, *24*, 3455−3460.
(39) Harris, M. R.; Li, Q.; Lian, Y.; Xiao, J.; Londregan, A. T. Construction of 1-Heteroaryl-3-azabicyclo[3.1.0]hexanes by sp3−sp2 Suzuki−Miyaura and Chan−Evans−Lam Coupling Reactions of Tertiary Trifluoroborates. *Org. Lett.* **2017**, *19*, 2450−2453.
(40) Hryshchuk, O. V.; Varenyk, A. O.; Yurov, Y.; Kuchkovska, Y. O.; Tymtsunik, A. V.; Grygorenko, O. O. gem-Difluorocyclopropanation of Alkenyl Trifluoroborates with the CF_3SiMe_3−NaI System. *Eur. J. Org. Chem.* **2020**, *2020*, 2217−2224.
(41) Grygorenko, O. O.; Babenko, P.; Volochnyuk, D. M.; Raievskyi, O.; Komarov, I. V. Following Ramachandran: exit vector plots (EVP) as a tool to navigate chemical space covered by 3D bifunctional scaffolds. The case of cycloalkanes. *RSC Adv.* **2016**, *6*, 17595−17605.
(42) Feskov, I. O.; Chernykh, A. V.; Kuchkovska, Y. O.; Daniliuc, C. G.; Kondratov, I. S.; Grygorenko, O. O. 3-((Hetera)cyclobutyl)-azetidines, "Stretched" Analogues of Piperidine, Piperazine, and Morpholine: Advanced Building Blocks for Drug Discovery. *J. Org. Chem.* **2019**, *84*, 1363−1371.
(43) Beak, P.; Wu, S.; Yum, E. K.; Jun, Y. M. Intramolecular Cyclizations of alpha-Lithioamine Synthetic Equivalents: Convenient Syntheses of 3-, 5-, and 6-Membered-Ring Heterocyclic Nitrogen Compounds and Elaborations of 3-Membered Ring Systems. *J. Org. Chem.* **1994**, *59*, 276−277.
(44) Rayner, P. J.; O'Brien, P.; Horan, R. A. J. Preparation and Reactions of Enantiomerically Pure α-Functionalized Grignard Reagents. *J. Am. Chem. Soc.* **2013**, *135*, 8071−8077.
(45) Li, J.; Burke, M. D. Pinene-Derived Iminodiacetic Acid (PIDA): A Powerful Ligand for Stereoselective Synthesis and Iterative Cross-Coupling of C(sp^3) Boronate Building Blocks. *J. Am. Chem. Soc.* **2011**, *133*, 13774−13777.
(46) Yoon, J.-M.; Lee, C.-Y.; Jo, Y.-I.; Cheon, C.-H. Synthesis of Optically Pure 3,3′-Disubstituted-1,1′-Bi-6-Methoxy-2-Phenol (BIPhOL) Derivatives via Diastereomeric Resolution. *J. Org. Chem.* **2016**, *81*, 8464−8469.
(47) Lehmann, J. W.; Crouch, I. T.; Blair, D. J.; Trobe, M.; Wang, P.; Li, J.; Burke, M. D. Axial shielding of Pd(II) complexes enables perfect stereoretention in Suzuki-Miyaura cross-coupling of Csp^3 boronic acids. *Nat. Commun.* **2019**, *10*, 1263.
(48) Danheiser, R. L.; Savoca, A. C. Applications of cyclopropylboranes in organic synthesis. 1. A stereocontrolled route to substituted cyclopropanol derivatives. *J. Org. Chem.* **1985**, *50*, 2401−2403.
(49) Renslo, A. R.; Jaishankar, P.; Venkatachalam, R.; Hackbarth, C.; Lopez, S.; Patel, D. V.; Gordeev, M. F. Conformational Constraint in Oxazolidinone Antibacterials. Synthesis and Structure−Activity Studies of (Azabicyclo[3.1.0]hexylphenyl)oxazolidinones. *J. Med. Chem.* **2005**, *48*, 5009−5024.
(50) Meijs, G. F.; Doyle, I. R. Reaction of gem-dibromocyclopropanes with potassium dimethyl phosphite in liquid ammonia. A highly stereoselective reduction. *J. Org. Chem.* **1985**, *50*, 3713−3716.
(51) Chen, C.; Kattanguru, P.; Tomashenko, O. A.; Karpowicz, R.; Siemiaszko, G.; Bhattacharya, A.; Calasans, V.; Six, Y. Synthesis of functionalised azepanes and piperidines from bicyclic halogenated aminocyclopropane derivatives. *Org. Biomol. Chem.* **2017**, *15*, 5364−5372.
(52) Hutton, H. M.; Schaefer, T. Proton Coupling Constants In Substituted Cyclopropanes. *Can. J. Chem.* **1963**, *41*, 684−689.
(53) The CCDC numbers for all of the X-ray crystal structures in this paper are given in the Supporting Information.
(54) Bajwa, J. S.; Chen, G.-P.; Prasad, K.; Repic, O.; Blacklock, T. J. Deprotection of N-tosylated indoles and related structures using cesium carbonate. *Tetrahedron Lett.* **2006**, *47*, 6425−6427.
(55) Ghosh, A. K.; Samanta, I.; Mondal, A.; Liu, W. R. Covalent Inhibition in Drug Discovery. *ChemMedChem* **2019**, *14*, 889−906.
(56) Wernevik, J.; Bergström, F.; Novén, A.; Hulthe, J.; Fredlund, L.; Addison, D.; Holmgren, J.; Strömstedt, P.-E.; Rehnström, E.; Lundbäck, T. A Fully Integrated Assay Panel for Early Drug Metabolism and Pharmacokinetics Profiling. *Assay Drug Dev. Technol.* **2020**, *18*, 157−179.
(57) Thorarensen, A.; Dowty, M. E.; Banker, M. E.; Juba, B.; Jussif, J.; Lin, T.; Vincent, F.; Czerwinski, R. M.; Casimiro-Garcia, A.; Unwalla, R.; Trujillo, J. I.; Liang, S.; Balbo, P.; Che, Y.; Gilbert, A. M.; Brown, M. F.; Hayward, M.; Montgomery, J.; Leung, L.; Yang, X.; Soucy, S.; Hegen, M.; Coe, J.; Langille, J.; Vajdos, F.; Chrencik, J.; Telliez, J.-B. Design of a Janus Kinase 3 (JAK3) Specific Inhibitor 1-((2S,5R)-5-((7H-Pyrrolo[2,3-d]pyrimidin-4-yl)amino)-2-methylpiperidin-1-yl)prop-2-en-1-one (PF-06651600) Allowing for the Interrogation of JAK3 Signaling in Humans. *J. Med. Chem.* **2017**, *60*, 1971−1993.
(58) Thorarensen, A.; Balbo, P.; Banker, M. E.; Czerwinski, R. M.; Kuhn, M.; Maurer, T. S.; Telliez, J.-B.; Vincent, F.; Wittwer, A. J. The advantages of describing covalent inhibitor in vitro potencies by IC50 at a fixed time point. IC50 determination of covalent inhibitors provides meaningful data to medicinal chemistry for SAR optimization. *Bioorg. Med. Chem.* **2021**, *29*, No. 115865.
(59) Ward, R. A.; Anderton, M. J.; Ashton, S.; Bethel, P. A.; Box, M.; Butterworth, S.; Colclough, N.; Chorley, C. G.; Chuaqui, C.; Cross, D. A. E.; Dakin, L. A.; Debreczeni, J. É.; Eberlein, C.; Finlay, M. R. V.; Hill, G. B.; Grist, M.; Klinowska, T. C. M.; Lane, C.; Martin, S.; Orme, J. P.; Smith, P.; Wang, F.; Waring, M. J. Structure- and Reactivity-Based Development of Covalent Inhibitors of the Activating and Gatekeeper Mutant Forms of the Epidermal Growth Factor Receptor (EGFR). *J. Med. Chem.* **2013**, *56*, 7025−7048.
(60) Meier, K.; Arús-Pous, J.; Reymond, J.-L. A Potent and Selective Janus Kinase Inhibitor with a Chiral 3D-Shaped Triquinazine Ring

https://doi.org/10.1021/jacs.5c08786
J. Am. Chem. Soc. XXXX, XXX, XXX−XXX

System from Chemical Space. *Angew. Chem., Int. Ed.* **2021**, *60*, 2074–2077.

https://doi.org/10.1021/jacs.5c08786
J. Am. Chem. Soc. XXXX, XXX, XXX−XXX